SiPM development and application for astroparticle physics experiments

H. Miyamoto*, **M. Teshima***, **B. Dolgoshein**†, **R. Mirzoyan***, **J. Nincovic***, **H. Krawczynski**‡

**Max-Planck-Institut für Physik, Föhringer Ring 6, 80805 München, Germany*
†Moscow Engineering Physics Institute, Kashirskoe Shosse 31, 115409 Moscow, Russia
‡Wash. Univ. in St. Louis, Phys. Dept. and McDonnell Center for the Space Sciences, 1 Brookings Dr., CB 1105, St. Louis, MO 63130, USA

***Abstract*. A Silicon Photomultipliers (SiPM/G-APD) is a novel solid state photodetector which has an outstanding photon counting ability. The device has excellent features such as high quantum efficiency, good charge resolution, fast response (<100 ps), very compact size, high gain (up to $2{\sim}3\times10^6$), very low power consumption with low bias voltages (30-70V), immunity to the magnetic field. In the last few years, UV sensitive SiPMs with a p-on-n structure have been developed by a few companies such as Hamamatsu, Photonique, Zecotek Photonics Inc., and institutes such as the MPI-HLL (Max-Planck-Institute for Physics - Max-Planck-Institute Semiconductor Laboratory) as well as the MPI-MEPhI (Max-Planck-Institute for Physics - Moscow Engineering Physics Institute) for astroparticle physics applications. Here the current status of the SiPM developments in the MPI-HLL, the MPI-MEPhI will be described. Also the study of SiPM applications to the focal plane detectors of the Imaging Atmospheric Cherenkov Telescopes (IACTs) MAGIC/MAGIC-II [1] and CTA [2], and the space-borne fluorescence telescope JEM-EUSO [3] will be reported.**

***Keywords*: Imaging Cherenkov, Imaging fluorescence, SiPM**

I. Introduction

A SiPM is an array of multiple avalanche Photodiodes (APDs), which are operated in Geiger mode. Each APD pixel is operated in binary mode, which outputs a fixed signal charge, regardless of the detected number of photons. The output signal from a SiPM is the total charge of all summed APD signals, which is proportional to the number of the detected incident photons.

The Photon Detection Efficiency (PDE) of a SiPM depends on the transmittance of the surface, the filling factor of the sensitive area, the quantum efficiency (QE), and on the Geiger efficiency of the device :

$$PDE = Transmittance \times Fill\_Factor \times QE \times Geiger\_Eff.$$

Drawbacks of this device currently is relatively low sensitivity to UV and blue light as well as a large dark current, optical crosstalk (OC) between micro-cells. To detect fluorescence and Cherenkov lights, high PDE in the UV region (from ∼300 nm to ∼400 nm) is essential. In the last few years, the MPI-MEPhI and the MPI-HLL have developed large area SiPMs ($3mm \times 3mm$) and matrices of them for astroparticle physics applications.

The high PDE of these devices will allow us to lower the energy threshold of MAGIC telescopes for the detection of gamma rays down to 10 - 20 GeV, and ensure the detection efficiency of JEM-EUSO for UHECRs with energies exceeding (2-3)$\times10^{19}$eV which will enlarge the overlap of the energy bands of JEM-EUSO and ground based detectors, such as Auger[4] and TA[5]. Also, the insensitivity to magnetic fields and the low power consumption of SiPMs are additional important advantages for space detectors.

II. Device developments at Hamamatsu, MPI-MEPhI, and MPI-HLL

Presently, we are considering the following three SiPMs for their application in the astroparticle physics experiments described above.

A. MPPC

The MPPC produced by Hamamatsu is the first commercial product of UV sensitive SiPM in the world. They achieved a relatively low dark rate (∼2MHz/mm^2 at 10°C for a product with 100 μm micro-cell pitch). Currently, the largest size of a general commercial product of this company is $3mm \times 3mm$. It will be difficult to assemble thousands of each pixels one by one for these telescopes, or even a few hundred times thousand pixels in the case of JEM-EUSO. Therefore, a special device of 16 ch (4×4) of 3mm × 3mm MPPC array in a ceramic package has been developed for our camera, which also reduces the dead space due to the packaging (See figure 1). This novel module is currently the largest size of a SiPM module in the world. Combining the module with a proper light funnel, an active detection area exceeding 85% can be achieved. As shown in the next section, MPPCs have higher sensitivities in the blue and green region than the UV region. To maximize the advantage of this device, we are also studying the use of a wavelength shifter. Thus, the device has an excellent promise to become the detector of choice for IACTs and fluorescence telescopes.

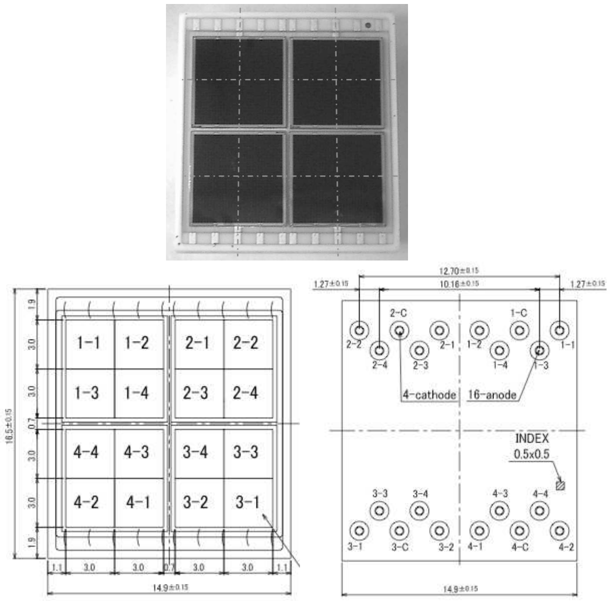

Fig. 1. Top : Photo of 16 ch MPPC array module. Bottom, Left/Right : Blue print of 16ch (4×4) of 3×3 mm^2 MPPC array device (front/back).

B. Dolgoshein SiPM

The SiPM developed by the MPI-MEPhI is called Dolgoshein SiPM after the name of the inventor. This device has a reasonably short output pulse with the width of ∼10 ns FWHM and a wide overvoltage range of $5 \sim 6$V. Since the PDE depends on the overvoltage, this wide range of overvoltage leads to an extremely high PDE. Currently the filling factor of this device is roughly 60% and the PDE reaches $> 50\%$ at 400 nm depending on the overvoltage. Also, this device has the advantage of the OC suppression. OC is a phenomenon when a micro-cell of SiPM generates photons that fire neighboring micro-cells. The OC may lead to an increased trigger threshold, especially in case of the telescopes operating in the presence of night sky background photons. There are two OC components. The "prompt" OC takes place when one or more photons directly hit a neighboring micro-cell(s) and trigger a breakdown like any external photon. The "slow" OC can be caused when a photon induces charge in neighbors bulk that subsequently migrates into the avalanche region. The OC is minimized by a design with an additional junction (a so-called double p-n junction) and with grooves between micro-cells that act as an optical isolation (See figure 2). The design leads to an OC suppression to a level of 3%.

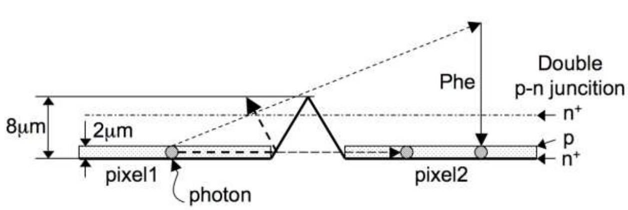

Fig. 2. Schematic view of "prompt" and "slow" optical crosstalk (OC) and the concept of OC suppression.

Currently, we have sample devices with several areas including a $3mm \times 3mm$ area device. A new device with even higher filling factor of around 70% and arrays of 4×4 and 8×8 devices are under development.

C. SiMPl

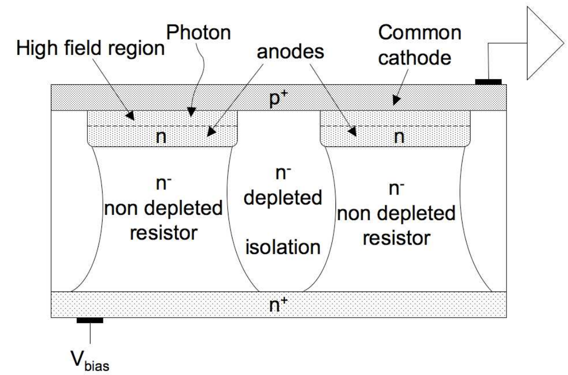

Fig. 3. Concept figure of bulk integrated quench resistor type SiPM (SiMPl).

The SiMPl developed by the MPI-HLL is a SiPM with a "bulk internal resistor". The device has a novel concept of a quench resistor integrated into the silicon bulk that enables not only to optimize the filling factor but also to simplify the production procedure. Therefore it has the potential to lower the cost and reduce the production time (see figure 3). Usually, one needs a polysilicon quench resistors on the surface of the device which cannot avoid producing a dead space on the entrance window and requires several involved fabrication steps. This design achieves a filling factor of ∼75%, a transmittance of the entrance window (with anti-reflecting coating) of 90%, a Geiger efficiency of 90%, and thus a quite high PDE of ∼61%. Devices of several sizes have been fabricated and tests on wafer level are ongoing. Also, the development of arrays of $3mm \times 3mm$ devices has started.

III. Toward the Application of SiPMs to Astroparticle Physics Experiments

There are some critical issues for the application of SiPMs in astroparticle physics experiments.

A. Sensitivity to UV and blue light

Figure 4 shows a schematic view of the PDE measurement setup. An LED located outside of the thermostatic chamber is flashed with an Agilent function generator at 2 kHz frequency. Three light sensors were tested in the wavelength range from 310 nm to 450 nm with different LEDs. The weak light from the LEDs was fed into a UV transparent fiber optic cable, the output of which was directed to a fused silica diffuser set at some distance from the sensors. The sensors tested in this measurement are Hamamatsu MPPC S10362-33-100C (3×3 mm^2 size, 100 μm micro-cell pitch), Dolgoshein SiPM (UV sensitive type, 3×3 mm^2, 100 μm micro-cell pitch), Hamamatsu R8900U-08-M36-MOD (1 inch 36

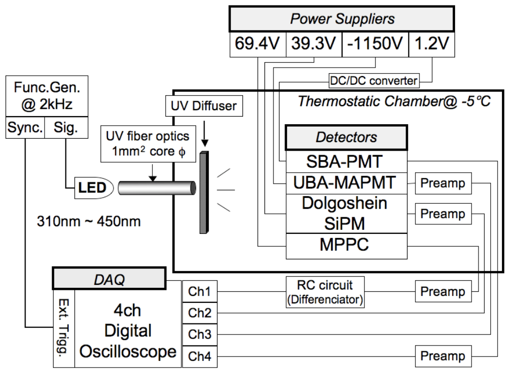

Fig. 4. Schematic diagram of the PDE measurement.

ch Ultra Bialkali - Multi Anode PMT (UBA-MAPMT) which is the device of the JEM-EUSO baseline design. The temperature inside the chamber is held at -5°C. The surface of R8900U-08-M36-MOD and the calibrated PMT R10408-MODULE are covered by a slit with a 3 mm x 3 mm square window to obtain the same aperture as that of the Dolgoshein SiPM and the MPPC. The LeCroy WavePro 7300A 3GHz Dual 20GS/s digital oscilloscope was used for the data acquisition. It was triggered by the synchronized signal from the function generator.

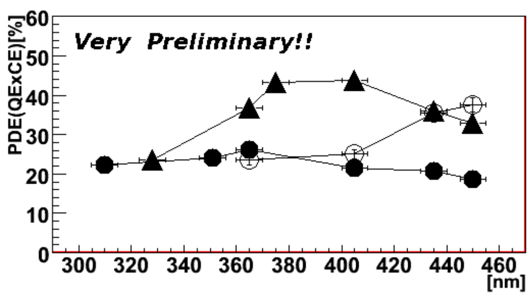

Fig. 5. Preliminary result of PDE measurements. The filled triangles, open circles, and filled circles show the distribution of the Dolgoshein SiPM, the MPPC, and the MAPMT respectively. The PDE is calculated from the ratio of the normalized number of detected photoelectrons in the considered device and in a reference PMT, assuming Poisson distributions. Systematic uncertainties are not shown. Other factors to be considered include the SiPM overvoltage and temperature dependence.

Preliminary results of PDE measurements

Figure 5 shows the preliminary result of the measured PDEs [%] as a function of wavelength [nm]. Assuming Poisson distribution, we calculated the ratio of the number of photoelectrons detected with the device under consideration and a reference PMT. The PDE is derived from the ratio described above multiplying by the QE and the collection efficiency (CE) of the reference PMT (95%). Although there are still some uncertainties concerning the absolute results, the relative results show the significantly higher efficiency of the SiPM from Dolgoshein compared to a MAPMT. Although the MPPC has a relatively low efficiency in the UV region, we are currently studying the efficiency of the method of using a wavelength shifter coating for enhanced sensitivity. Also, the PDE of SiPM depends on the overvoltage, and therefore even higher PDE is promising with higher voltage. The study of the PDE overvoltage dependence is ongoing.

B. Temperature dependence

Another critical issue for the SiPM application is its strong temperature dependence of the gain of -$3\% \sim -5\%/°C$. A temperature compensation circuit for the voltage supply with a thermistor can offer some solution. Thermistor is a resistor which has a temperature dependence that can be described as :

$$R = R_0 e^{B(1/T - 1/T_0)}$$

where R is the resistance of the thermistor at a temperature of T[K], B is a constant parameter (“B value”), and R_0 is the resistance of the thermistor at a reference temperature of T_0[K]. The figure 6 shows the schematic

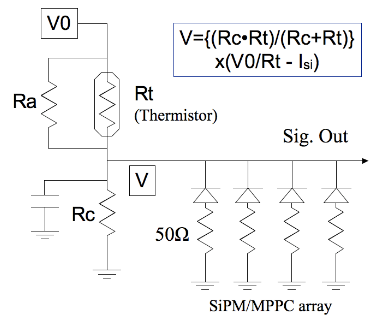

Fig. 6. Temperature compensation circuit with a thermistor (Rt).

view of the compensation circuit where V0 is a fixed initial voltage, and Rt is a thermistor. Using this circuit, we measured the gain and temperature of a MPPC by changing the ambient temperature from -18 °C to -8 °C. As a result, we obtained a gain drift of less than ±0.1 %/°C as shown in Figure 7. Figure 7 and 8

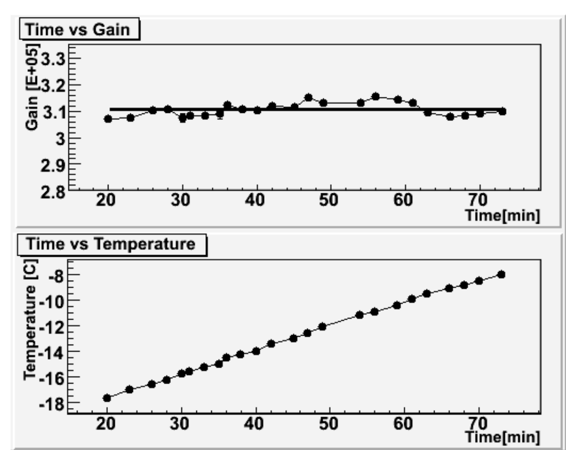

Fig. 7. The top panel shows the gain of a MPPC as a function of time [min] for a gradual increase of the device temperature [°C] (see bottom panel).

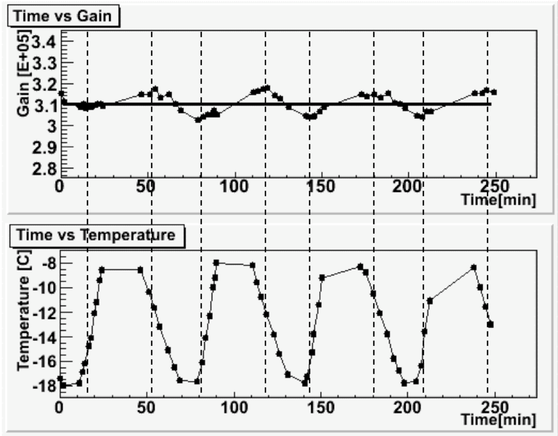

Fig. 8. The top panel shows the gain of a MPPC as a function of time [min] for a cyclic variation of the device temperature [°C] (see bottom panel).

show the MPPC gain [$\times 10^5$] as a function of time [min] for a temperature increase from -18 °C to -8°C (Fig. 7), and for cyclic temperature variations (Fig. 8). The latter temperature variations may be similar to the ones encountered when using the SiPM in space in a 90-min Low Earth Orbit (LEO). As one can see there the gain fluctuation is reduced to less than ±0.3 %/°C. The latter figure shows a time delay between the temperature change and the gain stabilization. Using a heat conductive glue, the heat conduction between the device and the thermistor should be higher and should lead to an even better gain stability.

IV. 256 CH PROTOTYPE CAMERA WITH 16 CH MPPC

We developed a prototype 256 ch MPPC camera consisting of 4 × 4 array of 16 ch MPPC modules. The camera design uses one mother board and four daughter boards. Socket pins for the signal readout and the bias voltage supply, and a thermistor are assembled on the mother board. The mother board is covered by a layer of copper to minimize the temperature variations across the camera. The daughter boards are oriented perpendicular to the mother board, and plug into four 20 pin board-to-board connectors. Each daoughter board reads out 64 ch, and includes the bias voltage supply with the temperature compensation circuit described above, and a shaper circuit. The design of the camera enables the separate modification of the mother and daughter boards (See photos in figure 9). For the readout of this camera, we use a CAEN VME 64 ch digitizer and alternatively, an ASIC currently under development for the JEM-EUSO readout system at RIKEN, Japan. The camera is presently used to study the trigger threshold, the temperature compensation of the gain, and electrical crosstalk.

V. SUMMARY AND OUTLOOK

UV sensitive SiPMs promise to be ideal sensors for IACTs and fluorescence telescopes. In this contribution, we report on the the status of the development of SiPMs for MAGIC, CTA, and JEM-EUSO projects. The PDEs

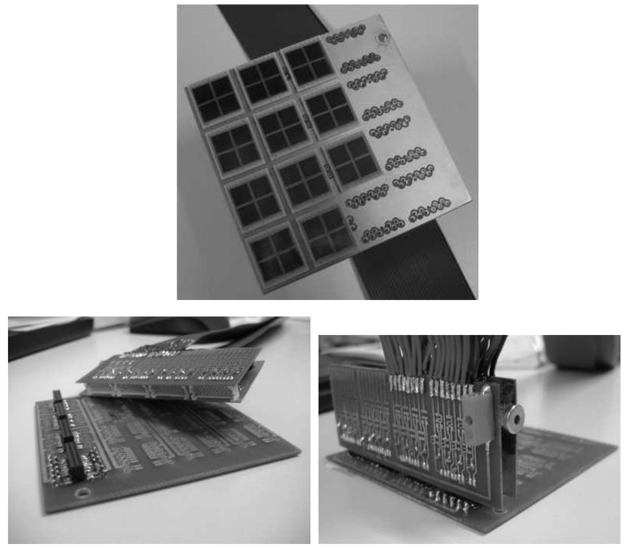

Fig. 9. 256 ch prototype camera with 4 × 4 MPPC array module. The circuit module consists of one mother board and four daughter boards to simplify the further modification.

of various SiPMs in the UV region have been measured. Further verifications of these results and additional measurements (e.g. of the overvoltage dependence of the PDE) are in progress. We have developed an MPPC 256 ch prototype camera for a Cherenkov telescope. We will be testing this camera in a small telescope which has a focal length of 1.5 m and a primary 60 cm diameter mirror. The telescope will be used to acquire images from Cosmic Ray air showers, and to study the trigger threshold and the night sky background event rate. After testing the camera with this small telescope, we will develop a camera cluster module for the MAGIC-II telescope. Furthermore, we are planning to develop a space-qualified detector module for the JEM-EUSO focal plane.

ACKNOWLEDGMENTS

We would like to thank all the technical and electronic staff of the MPI, the MEPhI, and the HLL for their contributions. We also acknowledge the MAGIC collaboration, the CTA consortium, and the JEM-EUSO collaboration. HK thanks the MPP for the hospitality during a sabbatical in spring 2009.

REFERENCES

[1] http://wwwmagic.mppmu.mpg.de/
[2] http://www.cta-observatory.org/
[3] http://euso.riken.go.jp/
[4] http://www.auger.org/
[5] http://www-ta.icrr.u-tokyo.ac.jp/
[6] P. Buzhan, et al., Proc. 5th International. Conf. on NDIP 2008, Palais des Congres, Aix-les-Bains, France, June 15-20 (2008).
[7] J. Nincovic, et al., Proc. 5th International. Conf. on NDIP 2008, Palais des Congres, Aix-les-Bains, France, June 15-20 (2008).